

Damage tolerance of an impacted composite laminate

N. Dubary, Christophe Bouvet, Samuel Rivallant, L. Ratsifandrihana

▶ **To cite this version:**

N. Dubary, Christophe Bouvet, Samuel Rivallant, L. Ratsifandrihana. Damage tolerance of an impacted composite laminate. Composite Structures, 2018, 206, pp.261-271. 10.1016/j.compstruct.2018.08.045 . hal-01880450

HAL Id: hal-01880450
https://hal.science/hal-01880450

Submitted on 14 Feb 2019

HAL is a multi-disciplinary open access archive for the deposit and dissemination of scientific research documents, whether they are published or not. The documents may come from teaching and research institutions in France or abroad, or from public or private research centers.

L'archive ouverte pluridisciplinaire **HAL**, est destinée au dépôt et à la diffusion de documents scientifiques de niveau recherche, publiés ou non, émanant des établissements d'enseignement et de recherche français ou étrangers, des laboratoires publics ou privés.



Open Archive Toulouse Archive Ouverte (OATAO)

OATAO is an open access repository that collects the work of some Toulouse researchers and makes it freely available over the web where possible.

This is an author's version published in: https://oatao.univ-toulouse.fr/21831

Official URL: https://doi.org/10.1016/j.compstruct.2018.08.045

To cite this version :

Dubary, Nicolas and Bouvet, Christophe and Rivallant, Samuel and Ratsifandrihana, Léon Damage tolerance of an impacted composite laminate. (2018) Composite Structures, 206. 261-271. ISSN 0263-8223

Any correspondence concerning this service should be sent to the repository administrator: tech-oatao@listes-diff.inp-toulouse.fr

Damage tolerance of an impacted composite laminate

N. Dubary[a,b], C. Bouvet[a,*], S. Rivallant[a], L. Ratsifandrihana[b]

[a] Institut Clément Ader, CNRS UMR 5312, Université de Toulouse, ISAE-SUPAERO – 10 av. E. Belin, 31055 Toulouse Cedex 4, France
[b] Segula Aerospace & Defence, Segula Technologies – Immeuble EQUINOX – bat. 1, 24 Boulevard Déodat de Séverac, 31770 Colomiers, France

Keywords:
Low-velocity impact
Damage tolerance
Compression After Impact (CAI)
Numerical modelling

A B S T R A C T

Composites are known to be vulnerable to out-of-plane loading such as impact. Investigating the residual properties of the laminate as a function of damage detection is the main purpose of impact damage tolerance design in aeronautics. As a good alternative to experimental campaigns, numerical approaches would lead to saving of time. The model developed in Institut Clément Ader over the last years enables representation of behavior of composite laminates subjected to low velocity/low energy impact – including permanent indentation – and Compression After Impact. Damage such as permanent indentation, fiber failures, matrix cracks and delamination are taken into consideration at each step thanks to a discrete ply modelling. The work presented here deals with the use of this model to make a composite laminate design optimization according to impact damage tolerance design. A method to improve optimization by reducing computation time is also proposed, based on a "best candidates" selection.

1. Introduction

Because of their high strength-to-weight ratio along with the will of using lighter structures, composites attract an increasing interest in many fields. However, their vulnerability to out-of-plane loading such as impacts leads to an over-dimensioning. Low velocity impacts can occur during manufacturing or operation on composite structures and can result in a significant reduction of the residual properties without visibly marking the surface. This external damage corresponding to the dent left by the impact event is called permanent indentation (PI). In aeronautics, requirements and design are based on the visibility of the damage (Fig. 1): under a certain level of detectability the structure should withstand ultimate loads; beyond this level the impacted structure should withstand limit loads without sudden failure until the detection of the damage during inspection. This level of detection is called "Barely Visible Impact Damage", or BVID [1–3], and is linked to the geometry, to the properties of the structure and to the impact energy. So even damaged and without detectability, the design should ensure that the structure bears in-service loads: this is the principle of damage tolerance. As a matter of fact, impact damage tolerance design of composite relies on two important parameters: residual strength and detectability of the impact given by the permanent indentation.

1.1. About modelling composites

From understanding to predictive work, many studies have been run on damage induced by Low-Velocity Impact (LVI) since 90's [2–9]. Analytical, semi-analytical models and formulations are the first approaches for predicting induced damage during quasi-static response or LVI and for characterizing residual properties of the structure [2–4,10–13]. For instance, critical load could be analytically determined to predict delamination growth [10]. Even if these approaches are quite efficient in certain domains, the complexity of the phenomena implies that numerical methodologies have to be developed. The FE method is a relevant approach to characterize the behavior of composite structures and to provide information on the impact damage phenomena. Reliable impact and Compression After Impact (CAI) simulations would be a valuable tool to replace tests and take place in the test pyramid [14,15]: this is the aim of virtual testing. The complexity of composites is that damage depend on the design of the laminate in terms of stacking sequence, ply thickness, nature of fibers, kind of reinforcement… driving to a different repartition of stress in the laminate and so to a reduction or an increase in stress location.

In order to have a faithful and reliable behavior of the laminate during simulation, it is necessary to sufficiently represent the events occurring during loading and damage development. These damage could be classified into two parts: intralaminar damage developed inside the ply (matrix cracking, fiber breakage or fiber/matrix debonding)

* Corresponding author.
E-mail address: christophe.bouvet@isae.fr (C. Bouvet).

https://doi.org/10.1016/j.compstruct.2018.08.045

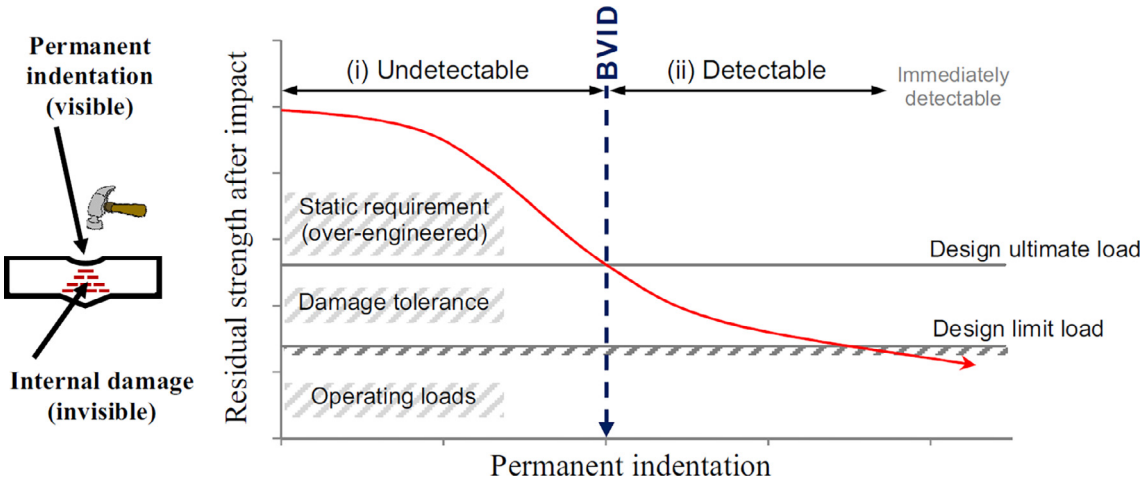


Fig. 1. Damage tolerance concept with detectable and undetectable damage.

and interlaminar damage developed at the interface between two plies, namely delamination. To have a good accuracy, the main damage captured by a numerical low velocity impact simulation are matrix cracking, fiber breakage and delamination [16 18] driving to a "relevant physics of the impact process" from under BVID to perforation range of impact [18].

Important research has been done on understanding, capturing and modelling delamination with good results [19 27], on the effect of delamination on the residual strength [28,29] showing a reduction of the residual strength in presence of delamination. Since the introduction of the cohesive zone model (CZM) in the 60's [30 32], delamination in composites is nowadays commonly simulated using cohesive elements and interface elements. For instance, interface elements are integrated in the model [16,33,34], and used with contact algorithms and friction between delaminated plies. Turon et al. [35] and Harper et al. [36] studied influence of cohesive zone interface strength parameters on mixed mode behavior. For instance, Harper et al. conclude that one should pay attention to the length of the cohesive zone on what depends the accuracy of the interfacial stresses. Relatively short length of the cohesive zone enables better results. Other approaches exist with Li et al. [23] who use fracture mechanics to simulate the delamination growth based on VCCT to evaluate the energy release rates. Or Menna et al. [17] who choose a modelling of the bond between plies through distributed spring connections, each ply being modelled by three dimensional eight node finite elements. Delamination is modelled by the use of a surface to surface tiebreak contact algorithm based on the knowledge of interlaminar properties (normal and shear strengths).

Concerning intraply damage modelling, fiber breakage and matrix cracking can be approached by continuum damage mechanics modelling with three dimensional solid elements including internal damage variables and a degradation of material properties following the direction as in [16,18,37]. All of these approaches are *meso* scale simulation strategies.

Faggiani and Falzon [33] propose a continuum damage mechanics approach for fiber breakage and matrix failure, each in tensile and compressive failure mode, using continuum shell elements. Modelling of matrix cracking using extended finite element method is also conducted by Iarve et al. [34]. This enables independence of the mesh orientation. Lopes et al. [18] also use cohesive elements in the ply between three dimensional elements in the material direction to capture matrix cracking. Likewise, de Moura and Gonçalves [25] place interface elements inside layers where matrix cracking is experimentally observed, implying the need of a previous study.

The importance of coupling between interlaminar and intralaminar damage is also admitted in literature [18,22 27,29,34,38]. The use of cohesive elements inside the ply in the material direction to capture matrix cracking and get a good coupling with the delamination is an other point to obtain accurate damage predictions. It is admitted that matrix cracking has a precursory role on delamination.

Then to estimate the residual strength and evaluate the damage tolerance of the laminate, interest is focused on modelling Compression After Impact with, for instance, some quite accurate models developed by Gonzalez et al. [39], Dang and Hallett [29], Tan et al. [40] or recently published by Panettieri et al. [41].

Gonzalez et al. [39] agree that the predictions deteriorate with an increasing number of layers. Their predictions are close to the experimental values, with a maximum relative error of 20% for the strength obtained during CAI.

Dang and Hallett [29] use a model that do not take into account fiber failure (impact are carried out at very low energy, and fiber failures do not occur or can be negligible in this case). During CAI, they link the compressive strength to the occurrence of significant delamination events.

Tan et al. [40] manage to capture both the qualitative and the quantitative aspects of intralaminar and interlaminar damage during impact and CAI. However they have little trouble to capture the good direction of delamination propagation, while having a good representation of the extended area.

Panettieri et al. [41] show the importance of the parameters of cohesive elements on the CAI result and on the computational cost. They point out that a compromise has to be made. They also admit than a reliable numerical approach could "not only lower the cost associated with the test but also enhance the design of composite structures".

Finally, related to the impact damage tolerance designing philosophy, attention is given to permanent indentation as a predictive mark to evaluate the residual capabilities of the structure [42]. This phenomenon is not well controlled yet, because it depends on several parameters: plate geometry, material, stacking sequence, impact energy or impactor shape, etc… and its origin is complex: local fiber failure [43], debris accumulation, local plasticity, etc.

Some formulations exist to integrate dent during impact test simulations: "plastic like" model included in the matrix behavior to take into account matrix cracking, plasticity and blocking debris [44], using anisotropic elasto plasticity theory [45], non linear shear of the intralaminar damage model [20,40] with combination of continuum theories of plasticity and continuum damage mechanics [37].

1.2. *Objectives of this study*

The Discrete Ply Model (DPM) developed at the Institut Clément Ader by Bouvet et al. makes possible to capture damage such as permanent indentation, delamination, fiber breakage and matrix cracks for

each step from the impact to the residual strength [44,46,47]. The DPM was validated by a test/simulation correlation for different stacking sequences in terms of delamination areas, force displacement curves and force time curves [46]. It also shows quite accurate results with dent depth and residual strength prediction [44,47], taking into ac count a certain experimental dispersion. Main details about the DPM approach and configuration are presented here after (Section 2).

From all of it, work with this model to propose an optimized la minate with an impact damage tolerance approach can be carried out. The classical design approach, according to damage tolerance concept, is to calculate the residual strength of a wide range of laminates for a damage very close to BVID, to determine the best laminate, i.e. with the highest residual strength at BVID. A classical optimization loop can be used. Indeed, when the damage is barely visible, residual strength can be reduced by 50% while the standards require the structure to with stand ultimate loads (Fig. 1): this moment is a crucial point in designing laminate structure. This is the key point of the presented approach: the capability of using the model to capture BVID impact energy, and then obtain the associated residual strength.

After a brief recall of the DPM and the numerical modelling used, an experimental validation of the global impact and CAI simulation on a few laminates will be done, to validate the use of the model for the design optimization study.

Then, the method proposed for this design optimization is presented and applied to a set of laminates to determine the one with the highest residual strength according to damage tolerance. A way to improve computing time efficiency is also presented, based on a selection of best laminate candidates, to avoid running too many time consuming si mulations on unnecessary cases.

2. Numerical modelling: Description and validation

The model of composite damage used in this study, named "Discrete Ply Model" (DPM), was extensively presented in [44,46,47]. This model is used with a VUMAT law and run with Abaqus/explicit. Only a brief recall is done in order to allow a better understanding of the model and the interested reader can find more details in [46]. Here are exposed the modelling of the different damage, a focus on the permanent indenta tion, and the material and boundary conditions used. Then, an ex perimental validation is presented.

2.1. Element formulation and behavior laws

The principle of the DPM is to simulate the major failure modes observed in composite impact tests (delamination, matrix cracking and fiber failure) as follows (Fig. 2):

- The delamination is simulated using classical interface elements between two consecutive plies; each ply being modelled with one volume finite element in the thickness. Then the damage in the delamination interface elements is classically driven using fracture mechanics. One more consideration is a communication with the volume element and the local effect that fiber failures could have on close interfaces.
- The intra ply matrix cracking is simulated with interface elements normal to the transverse direction. The damage in the matrix cracking interface elements is driven using Hashin's Criterion cal culated in neighboring volume elements (Eq. (1)):

$$\left(\frac{\sigma_t^+}{\sigma_t^f}\right)^2 + \frac{\tau_{lt}^2 + \tau_{tz}^2}{(\tau_{lt}^f)^2} \leqslant 1 \tag{1}$$

with (l, t, z) the orthotropic directions, σ_t^f the transverse failure stress and τ_{lt}^f the shear failure stress. The second part of the law is based on the same formulation as for delamination criteria. Even if matrix cracks are not detrimental for residual strength, delamination is usually linked to it. These interface elements constrain to a complex mesh, but allow to naturally obtain the coupling between intra and inter laminar da mage. This coupling is known as crucial to simulate the complex da mage morphology developing in composite structures during impact [18,22 27,29,34,38].

- Fiber failure is considered through conventional continuum damage mechanics but with an original formulation between the integration points of the element to take into account the crack surface energy with a bilinear material law inside the volume (Eq. (2)). This ap proach can be compared to methods based on characteristic element length which makes mesh size independent modelling possible.

$$\int_V \left(\int_0^{\varepsilon^1} \sigma_l d\varepsilon_l \right) \cdot dV = S \cdot G_I^f \tag{2}$$

where G_I^f is the energy release rate in opening mode in fiber direction, V and S are element volume and section, σ_l and ε_l are longitudinal stress and strain, and ε^1 is the strain at total degradation of fiber stiffness.

Once strain of damage initiation in tension ε_t^0 or in compression ε_c^0 is reached, a damage variable corresponding to a linear decrease of the stress is calculated and stresses are determined from the damaged or thotropic elastic stiffness matrix. In compression, a plastic behavior is also considered for highest strains and a crushing stress σ^{crush} [48] is applied as a plateau.

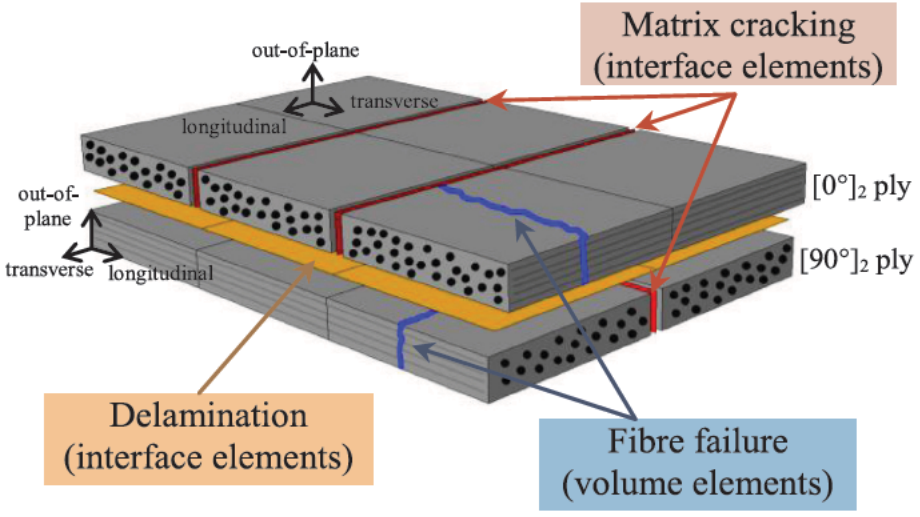


Fig. 2. DPM principles: element types and associated damage.

Menna et al. talk about the mesh dependency of the result: “the composite material failure behavior is influenced by the element size affecting the absorbed energy which varies with the element length and converges for small element dimensions” [17]. They use elements of approximatively 0.657 mm size. In our case, to obtain a good propagation of the last interface delamination (at the non impacted face), the mesh is reduced to 0.833 mm size elements. It also has to be noticed that the thickness of elements is smaller than during previous validation of the model (0.25 mm against 0.5 mm) [46], and the number of interfaces is increased causing a more complex model. It was observed that the result is more reliable when the element length is smaller. To avoid excessive time calculation, this size of 0.833 mm is the limit of the model to get a good delamination: beyond this size the propagation at the last interface does not occur.

2.2. Permanent indentation modelling

As previously seen, the permanent indentation is the mark left onto the surface after an impact event. It is defined as the difference in a direction normal to the face of the specimen between the lowest point in the dent and the surface that is undisturbed by the dent [49]. Its origin is not well controlled yet, but previous studies show that it is mainly linked to fiber breakage, matrix plasticity, or blocking debris [41]. In the model, it is represented thanks to a pseudo plastic non return law in intra ply interface elements.

The capability of DPM to represent permanent indentation is validated by the curves return during impact unload (in impact force displacement curves). It is to be noticed that this model does not take into account the natural relaxation of the plate after impact: the permanent indentation value reduces during a couple of days following an impact event by elasticity behavior. For this reason, all measures of experimental permanent indentation value are carried out at least 48 h after impact tests and could be smaller than the numerical ones measured at the end of impact simulation.

2.3. Material and boundary conditions

The model is so used to simulate experimental impact and CAI tests on $4 \times 100 \times 150\,mm^3$ rectangular laminate plates of T700/M21 UD carbon/epoxy composite. Properties used in the model are presented in Table 1. The number of plies is fixed at 16 plies of 0.25 mm thickness. Orientations in the stacking sequence are limited to 0°, ± 45° and 90° with the same fiber percentage for each direction. Considering symmetrical reasons, only a half plate is meshed. The boundary conditions are given by the contact between the plate and a fixed rigid body, representing experimental condition tests presented hereafter (Fig. 3).

For the impact test, the plate is supported by a $75 \times 125\,mm^2$ window and is impacted at its center by a 2 kg hemispherical impactor of 16 mm diameter, numerically assumed non deformable (Fig. 3a). Following the impact, a relaxation step is simulated. This step put the plate in quasi static state by eliminating major vibrations and waves induced by the impact event. During this step CAI boundary conditions are also set up. According to the ASTM D7137/D7137M standards [50], they consist of two longitudinal stabilizing knives spaced 90 mm and two clamping blocks at the lower and upper sides of the plate spaced 130 mm (Fig. 3b).

Table 1
Material properties used in the model.

E_l^t (GPa)	E_l^c (GPa)	E_t (GPa)	ν_{lt}	G_{lt} (GPa)	G_{tz} (GPa)
130	100	7.7	0.3	4.75	2.9
σ_t^f (MPa)	τ_{lt}^f (MPa)	σ^{crush} (MPa)	ε_t^0	ε_c^0	
60	110	250	0.018	0.0125	
$G_{I,c}^d$ (N/mm)	$G_{II,c}^d$ (N/mm)	G_t^f (N/mm)	G_c^f (N/mm)		
0.4	1.8	130	10		

2.4. Experimental validation

A previous validation of DPM capability to represent both impact and CAI has been done and presented in [46]. Validation was based on experimental/numerical comparisons of delamination (C scan), impact force/displacement curves and CAI strengths from various laminates with 0.5 mm thickness plies (0.5 mm plies in the numerical simulation, two 0.25 mm combined plies in the experiments).

During this study, new tests were done to validate the model with 0.25 mm thickness plies, in order to be able to simulate more realistic laminates. They consist in 25 J impact and CAI tests on $4 \times 100 \times 150\,mm^3$ laminates made of T700/M21 UD tapes. ASTM D7137/D7137M standards were used, and 6 specimens tested: 3 different stacking sequences, tested twice for repeatability.

A: $[45/-45/90/0/90/0/45/-45]_S$
K: $[45/-45/0/45/-45/0/90_2]_S$
O: $[45/-45/45/-45/90/0/90/0]_S$

Fig. 4 presents impact force/displacement curves for the three A, K and O specimens: two experimental curves for each specimen, and the associated simulation. A very good agreement was found for all three cases, both during loading and unloading phases.

To have more comparison data, C scan were also performed for one of each specimen type. The obtained delamination maps are also presented on Fig. 4, beside delamination coming from the numerical simulation. Specimen A and K present good correlations, with very good numerical estimations of the delaminated interfaces, shapes and areas.

Finally, permanent indentations (Fig. 5a) were also measured 48 h after the end of impact tests, using digital image correlation. They are in accordance even if the numerical results are overestimated. One can explain this difference with the relaxation phenomena causing too high numerical permanent indentation value. Moreover, the evolutions of permanent indentation from one specimen to another are the same in experiments and simulations. At this level of modelling, it can be assumed that the result is good.

Importance is finally given to the residual strength got during CAI on the three stacking sequences A, K and O. Fig. 5b shows that, even if, like for permanent indentation, the results are slightly overestimated (10 15%), the ranking in terms of performance is well represented. This means that the simulation is also able to give a hierarchy in terms of layups strength capacity, which is the most important in design when searching for the best laminate.

3. Numerical approach: Laminate design optimization with impact damage tolerance

3.1. Classical approach

Previous work and results presented first in this article show that the DPM model is advanced enough to propose an impact damage tolerance design approach. A classical numerical design approach would be to cover the laminate design space by changing stacking sequences, materials, number of plies, and calculate residual stress at BVID. As the concept of damage tolerance in composite is based on the visibility of the damage (residual strength is calculated at BVID), the optimization loop is based on an inner loop to determine the impact energy level to obtain a permanent indentation (PI) equal to BVID (Fig. 6). This inner loop does not necessitate the full impact and CAI calculation as the permanent indentation is calculated at the end of the impact energy and the CAI calculation is run only for the BVID energy

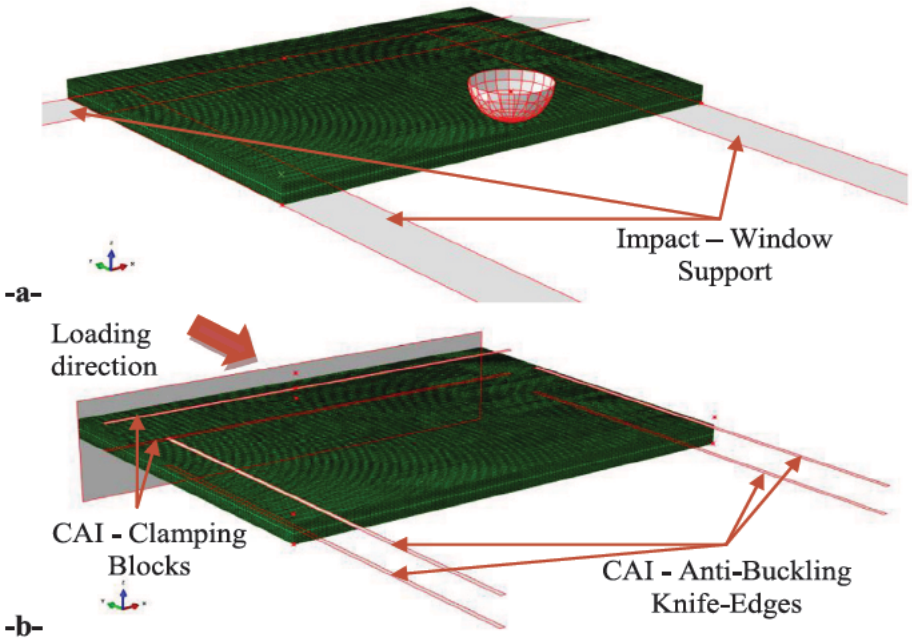


Fig. 3. Impact (a) and CAI (b) boundary conditions of the model.

level.

However, the design space must be totally covered, and the main drawback of this approach is the necessity to run several impact calculations to converge towards the BVID energy for each candidate laminate. To decrease computation time, the idea developed hereafter is to take into account the evolution of CAI/PI curve to determine a limited set of "best candidates" on which the overall optimization loop will be run. But before, it is necessary to have a sufficient knowledge of the CAI/PI curve behavior, studied in the following sections.

3.2. Configuration of the study and laminate sampling

As recalled in Section 2.4, the first model validation tests have been run on double plies (0.5 mm thick) stacking sequences based on a variation of the reference $[0/45/90/-45]_S$. It has been noted that laminates containing thinner plies are more impact damage tolerant even placing $45/-45^\circ$ plies in external position from the presented reference case. Therefore, in this study, layups closer to industrial laminates, with 0.25 mm thick plies are considered.

As the objective of this study is to show that it is possible to make a design optimization thanks to damage tolerance philosophy with the DPM, only a reasonable number of simulations have been done, to limit the overall calculation time. The first choices were to fix the number of plies to 16, to use only 0°, 90° and ± 45° plies, and to follow the classical stacking rules: quasi isotropic laminate, mirror symmetry, and a set of ± 45° external plies to increase buckling strength. It was also chosen to keep together +45° and −45° plies whatever their location in the thickness. Within the possible configurations, only 18 cases were finally investigated (Table 2), and the reference case (REF) was also added to the numerical simulation campaign. It includes the 3 cases (A, K, O) presented above for the experimental validation.

3.3. Full impact and CAI calculation approach

Instead of a classical optimization loop, in order to understand the CAI/PI curve evolution, full impact and CAI simulations have been done at different energy levels. It will permit to propose an alternative method of optimization in a further section.

3.3.1. First step: 25 J impact and CAI simulation results

The first step consists in a 25 J impact and CAI simulations campaign on the 19 stacking sequences exposed in Table 2. The energy of 25 J is chosen according to the standards ASTM D 7136/D 7136 M specifying that impact energy is 6.7 J/mm times the nominal thickness of the specimen (given 26.8 J). Each simulation is accomplished in around 36 h on 20 CPUs. Mainly force displacement curve, delamination area, PI and CAI stress are extracted for each laminate for impact and CAI. For brevity, only parts of these results are exposed here: PI (Fig. 7a) and CAI stresses (Fig. 7b).

Fig. 7a shows that with the 25 J energy determined from the norms, all calculated permanent indentations are below the detectability level. Moreover, permanent indentations vary in a wide range: from 0.14 to 0.44 mm. Fig. 7b also shows a great dispersion in residual stress, from 200 to 250 MPa.

The first conclusion of these results is that the sampling of laminates chosen is wide enough to present various PI and CAI stress values.

The second point is that it is not possible to determine the best laminate i.e. the best residual strength at BVID from this unique set of 19 calculations at 25 J.

To go further in this analysis, the CAI stress versus PI curve was plotted (Fig. 8). Even if it is known that the CAI strength decreases when energy and permanent indentation increase [47], it is not sufficient to determine which laminate will have the highest residual strength at BVID. For example, looking at cases A and REF on Fig. 8: REF has a lower residual strength compared to A, but a higher damage visibility. A low decrease of CAI stress with increase of PI (red dashed arrows) will favor laminate A (i.e. highest residual strength at BVID), while a high decrease (red dotted arrows) will favor laminate REF.

It is then necessary to make new simulations, at higher energy levels, to study the evolution of CAI stress versus PI.

3.3.2. 2nd step: Higher impact energy levels

In order to be closer to the detectability level (BVID), impacts at higher energies are so simulated for each laminate. Firstly, intermediate energy is chosen case by case (in red in Fig. 9), adjusted from first results: the goal being a permanent indentation close to the 0.5 mm BVID. Seeing that some permanent indentations were still distant from BVID value, a third impact campaign was carried out at 40 J for all

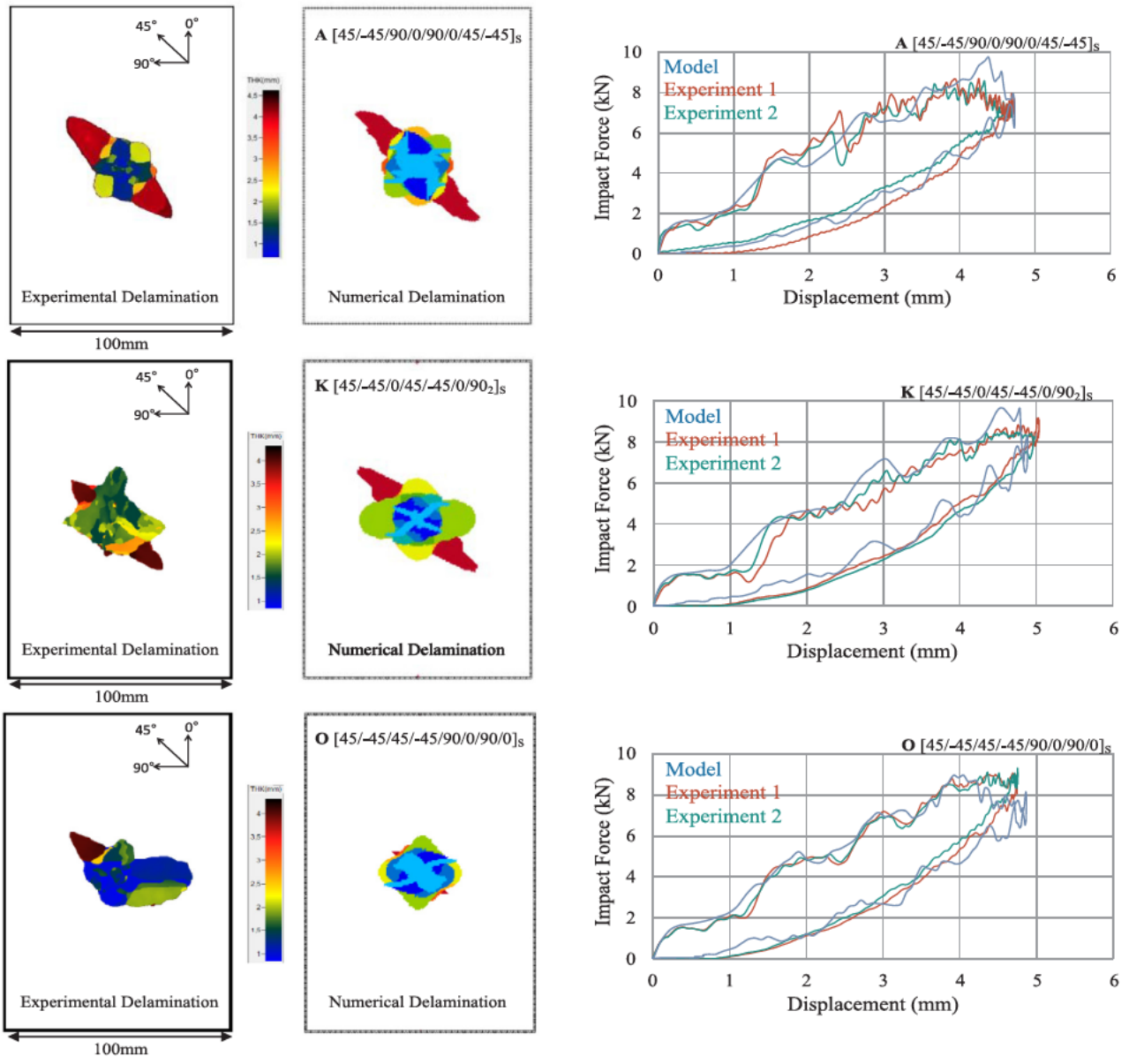


Fig. 4. Experimental/numerical comparison of 25 J impact results for A, K and O layups: C-scans and force/displacement curves.

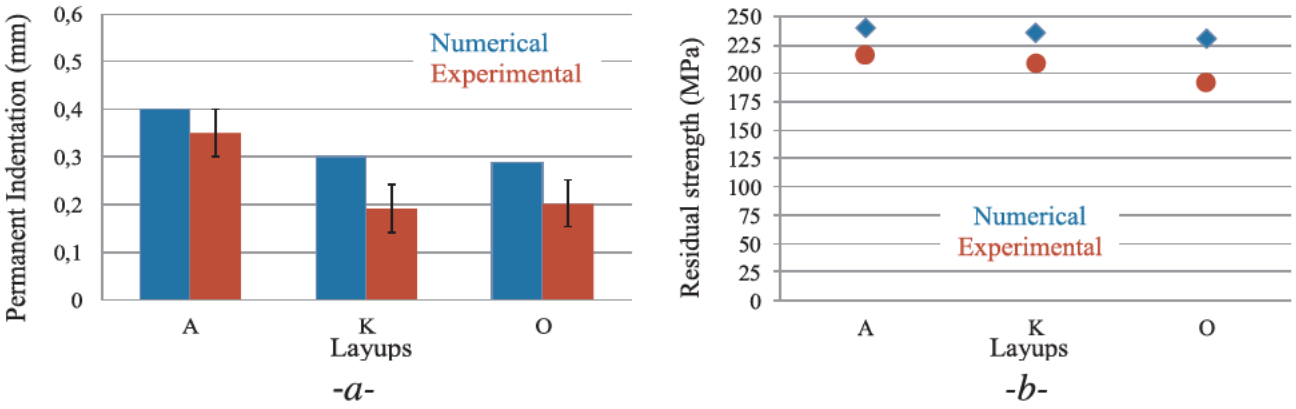


Fig. 5. Experimental/numerical comparison of permanent indentation (a) and residual strength (b) for A, K and O layups after 25 J impact.

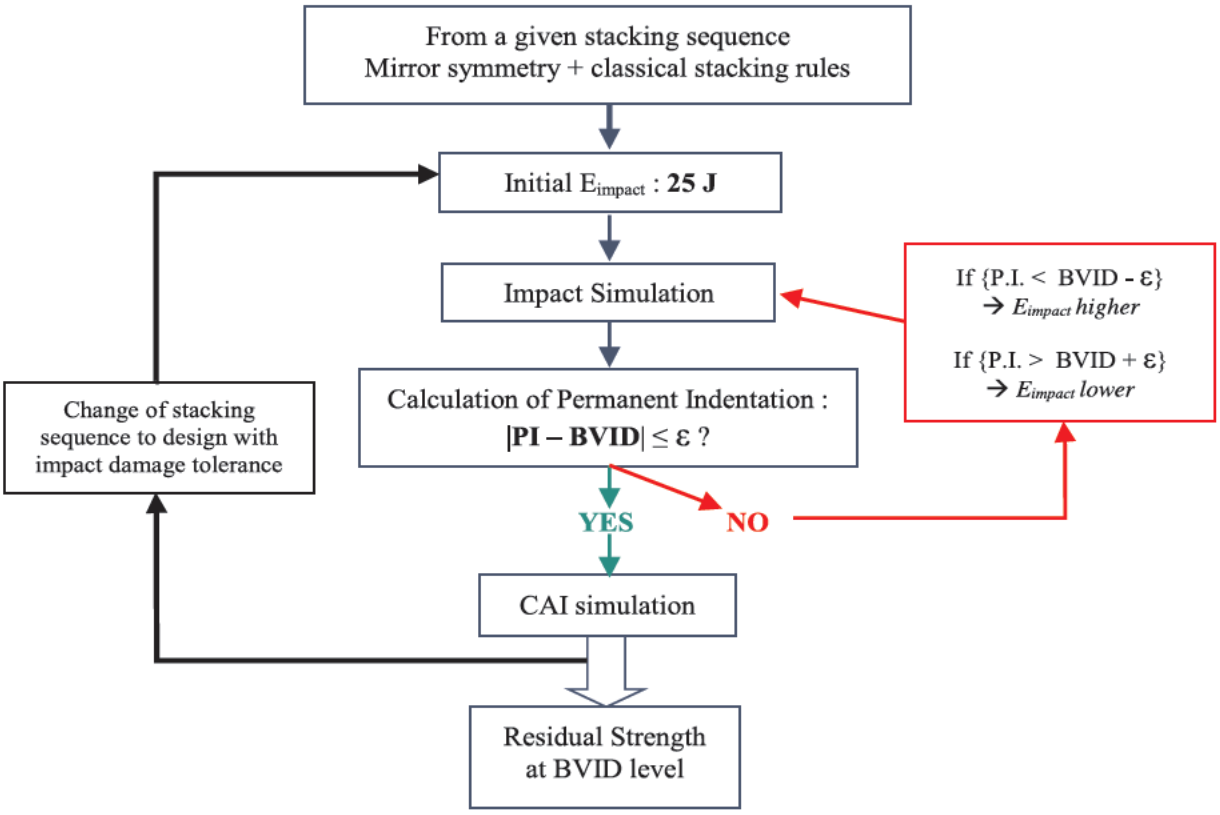


Fig. 6. Classical optimization loop for numerical design of composite laminates with damage tolerance approach.

laminates. From these studies, permanent indentation (Fig. 9a) and residual strength (Fig. 9b) were recorded.

From these results, it also emerges that the model has globally a faithful behavior: permanent indentation and residual strength are respectively higher and lower with an increase in impact energy. Exception done for some cases: slightly smaller values of permanent indention for laminate *REF* between 25 J and 28 J or laminate *E* between 32 J and 40 J and higher value of residual strength for laminate *I* (*M*) between 35 J (37 J) and 40 J. Due to the complexity of the model, the existing dispersion in experiments and the close values of impact energies, these phenomena are not questioned but are taking into account during the discussion of this study.

These new impact energy levels giving permanent indentation values close to BVID, it is possible to use a linear interpolation between the two calculation points surrounding BVID (or slight extrapolation in cases where BVID is not reach even at 40 J) to have a quite good estimation of the impact energy leading to BVID for all laminates.

And from these estimated energy values, an interpolation can also be done to determine the CAI stress at BVID. Fig. 10 presents these values, and show that at BVID, laminates *I*, *E*, *F*, *A* and *H* are the best structures in terms of impact damage tolerance design, with a residual stress superior to 230 MPa, that is more than 20% higher to the lowest value of the 19 tested laminates.

Of course, to obtain these results, it was not necessary to run calculation for all laminates and energies both for impact and CAI. It would have been more time efficient to run only impact test to determine BVID energy by interpolation, and then to run only one CAI simulation per laminate. But, it was chosen to do it that way to have also information on the evolution of CAI versus PI curves, in order to propose a more efficient method to optimize laminate design with damage tolerance philosophy.

4. Method improvement: "Best candidates" approach

4.1. Description of the "best candidates" approach

The evolution of CAI with PI from the three impact energy levels for some of the tested laminates is presented in Fig. 11. Only 9 curves are plotted for a matter of readability. It shows the global decrease of residual stress when permanent indentation increases, but also that the decrease slope is not uniform, depending on the laminates. The distribution of slope values, calculated from the 19 laminates, is given in Fig. 12. There are two ways to calculate these slopes: the average slope calculated with the three energy levels, and the slope calculated only from the initial (25 J) and final (40 J) energy levels. As can be seen on the distribution graph (Fig. 12), results show a quite small difference

Table 2
Stacking sequences studied.

	REF – $[0_2/45_2/90_2/\ 45_2]_S$	
A – $[45/\ 45/90/0/90/0/45/\ 45]_S$	*B* – $[45/\ 45/90/0_2/90/45/\ 45]_S$	*C* – $[45/\ 45/0/90/0/90/45/\ 45]_S$
D – $[45/\ 45/0/90_2/0/45/\ 45]_S$	*E* – $[45/\ 45/0/90/45/\ 45/90/0]_S$	*F* – $[45/\ 45/0/90/45/\ 45/0/90]_S$
G – $[45/\ 45/90/0/45/\ 45/0/90]_S$	*H* – $[45/\ 45/90/0/45/\ 45/90/0]_S$	*I* – $[45/\ 45/90/45/\ 45/90/0_2]_S$
J – $[45/\ 45/90/45/\ 45/0_2/90]_S$	*K* – $[45/\ 45/0/45/\ 45/0/90_2]_S$	*L* – $[45/\ 45/0/45/\ 45/90_2/0]_S$
M – $[45/\ 45/45/\ 45/90_2/0_2]_S$	*N* – $[45/\ 45/45/\ 45/0_2/90_2]_S$	*O* – $[45/\ 45/45/\ 45/90/0/90/0]_S$
P – $[45/\ 45/45/\ 45/0/90/0/90]_S$	*Q* – $[45/\ 45/45/\ 45/90/0_2/90]_S$	*R* – $[45/\ 45/45/\ 45/0/90_2/0]_S$

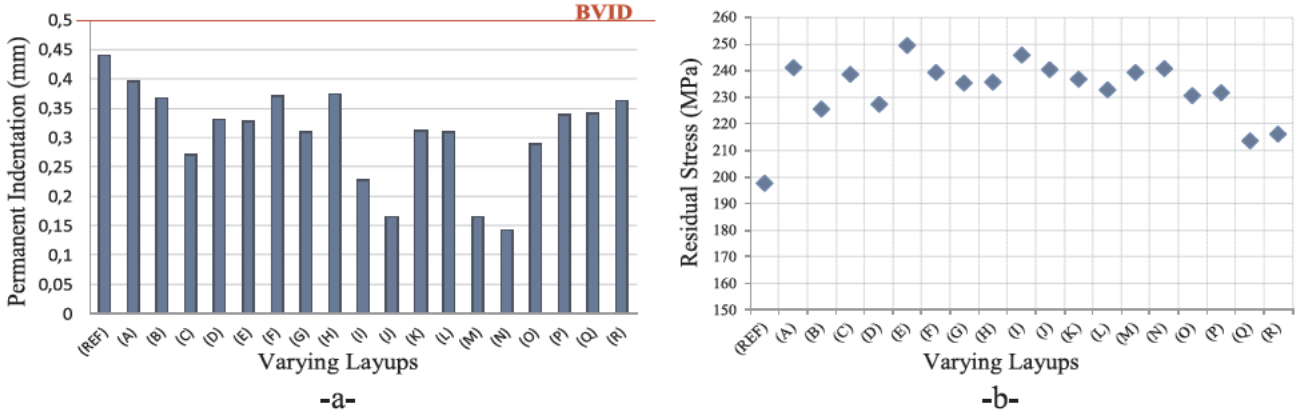


Fig. 7. 25 J impact and CAI simulations: (a) Permanent indentation – (b) CAI stress.

between these two methods, and the slope varies from approximatively −150 MPa/mm to −25 MPa/mm, with a peak of distribution between −70 and −45 MPa/mm.

From these observations, it is possible to propose a method to de crease the number of simulation during the design optimization, by selecting a set of "best candidates" directly from a first impact and CAI simulations campaign on all the laminates considered. Fig. 13 illus trates this method. The five points correspond to a first energy level simulation. This energy can be calculated from the standards re commendations, but it is not necessary to choose the same energy level for the different laminates. From these first results, a linear extrapola tion of CAI stress is calculated at BVID. As represented on the graph with the two arrows for each point, the distribution in slope presented above is taken into account in the estimation, giving inferior and su perior values. The example given here shows that laminates 1 and 2 have the highest CAI stresses estimated at BVID.

This method of "best candidates" being based on an estimation of CAI at BVID from a first simulation at a given energy, the estimation will be as better as the first permanent indentation values obtained are close to the BVID.

It should also be noted that the example in Fig. 13 shows results of first simulations with permanent indentations lower than the BVID, but the method works the same if permanent indentation is superior to BVID.

4.2. "Best candidates" approach applied to the 19 samples: Results and discussion

The "best candidates" method is applied to the set of 19 laminates presented in Section 3.2. The 19 first simulations are done for a 25 J impact energy, as recommended by the standards. The estimation of CAI at BVID is done from the knowledge of CAI versus Permanent In dentation slope distribution. Of course, we used here the results of the full simulations at different energy levels to calculate this distribution, which is not possible when the study starts from zero. This distribution evaluation should be done from a few calculations with random lami nates at two different energy levels. It is not necessary to make calcu lations for all laminates, the idea being to have the minimum re presentative sampling of laminates on which to turn full impact and CAI simulations.

Fig. 14 shows the method applied to 25 J initial simulations for the 19 laminates. Black arrows represent the linear decrease with the minimum value of slope ("low" decrease) taken from the distribution law. The red arrows ("high" decrease) correspond to the maximum slope. Looking only the high decrease, the graph shows that the highest estimated residual stress at BVID is obtained for laminate E, with 230 MPa. Thus, no laminate with a CAI stress estimation at BVID with low decrease inferior to 230 MPa, can be the best laminate. Here, all "best candidates" laminates are represented by the points above the black arrow coming from the point corresponding to laminate J, ending at 230 MPa at BVID. Best candidates are then E, A, I F and H, like found in the previous full study (Section 3.3), and also laminates C and K.

This method enables limitation of the study from 19 laminates to 7.

The method has also been applied to all laminates starting from 40 J energy, and starting from the intermediate energies given in Section 3.3. Results are nearly the same for the composition of the group of best candidates, and the five laminates A, E, F, H and I are always in these groups.

After this selection of a reduced number of candidates, the step is the research of the laminate with the best residual stress at BVID. This

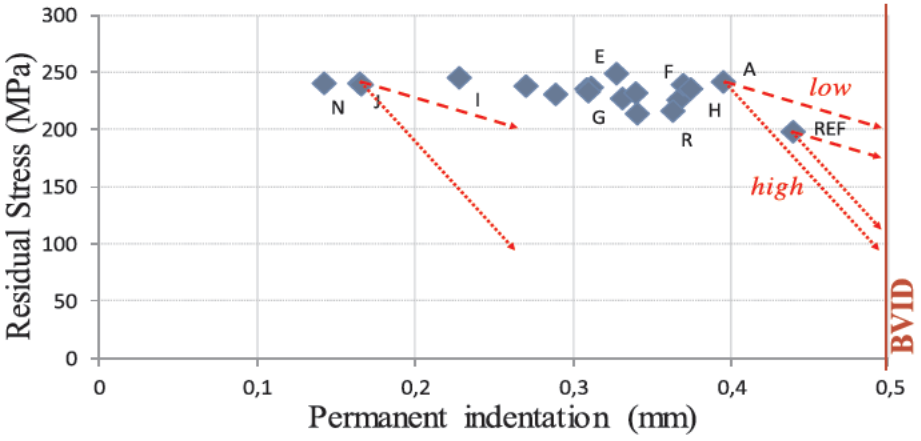


Fig. 8. CAI stress in function of permanent indentation for each layup impacted at 25 J.

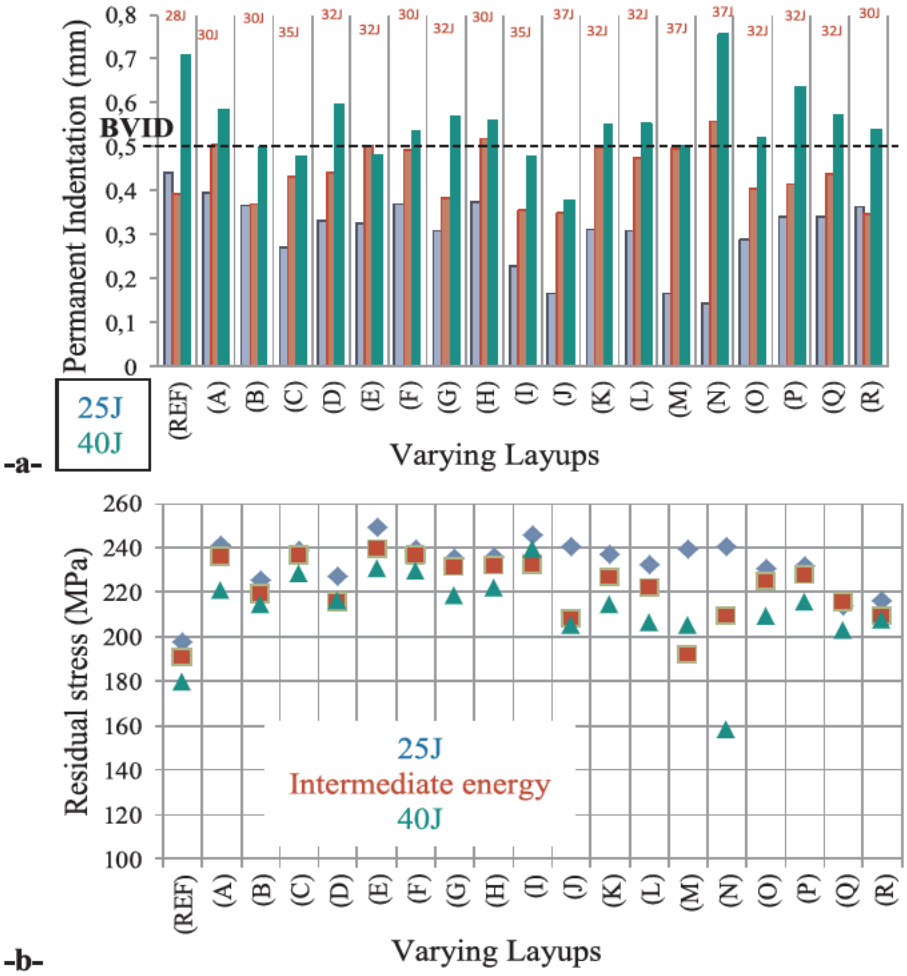


Fig. 9. (a) Permanent indentation and (b) residual stress of the different layups at 25 J, intermediate energy and 40 J.

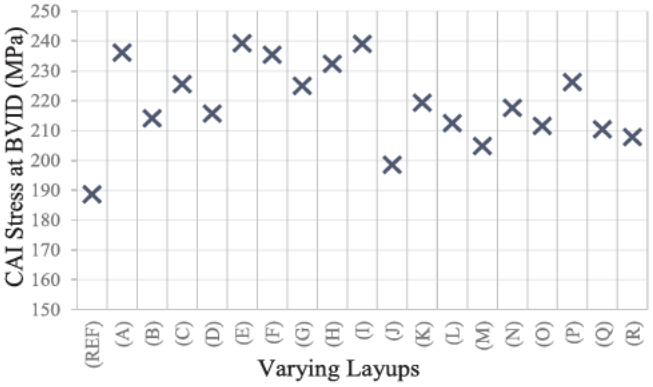


Fig. 10. CAI Stress at BVID calculated by interpolation, for all laminates.

step can be done with a classical optimization loop as presented in Section 3.1, or in the same way as presented in this paper at Section 3.3. For both cases, the reduced number of laminates studied leads to a reduction in the full computation time of the design optimization, and the benefit increases with the number of laminate to take into account during the design optimization. The interpolation method will of course give the same results as found in Section 3.3, as it is exactly the same study, with the same calculations, but reduced to 7 laminates (that is why the results are not presented here a second time).

After presenting these different ways to make the numerical design optimization of a composite laminate under damage tolerance, it is

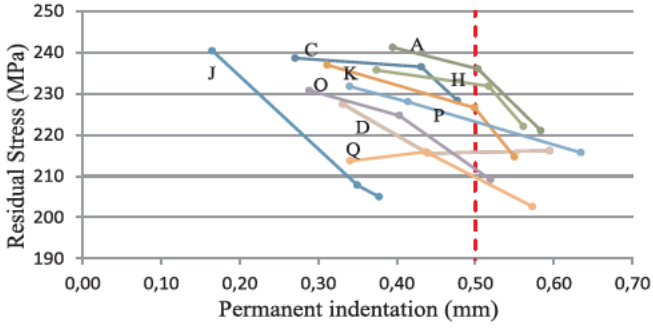


Fig. 11. Evolution of CAI stress with permanent indentation.

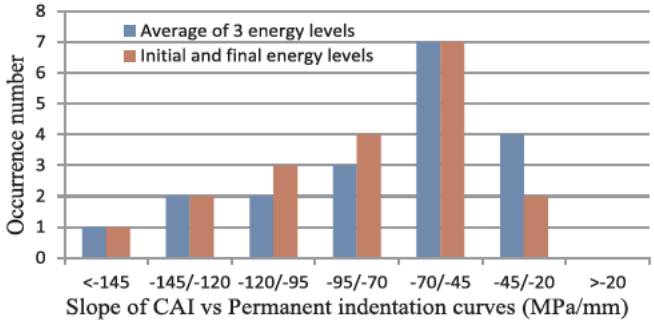


Fig. 12. Distribution of the slopes of CAI vs PI curves.

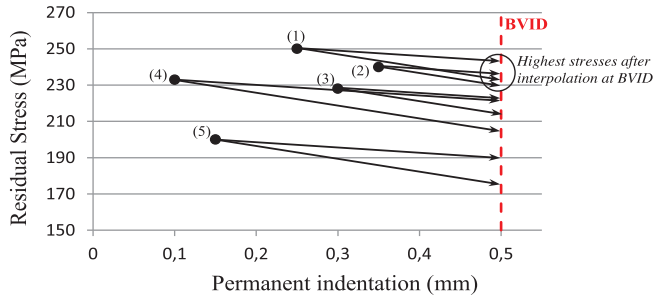


Fig. 13. "Best candidates" method: principle of CAI estimation at BVID.

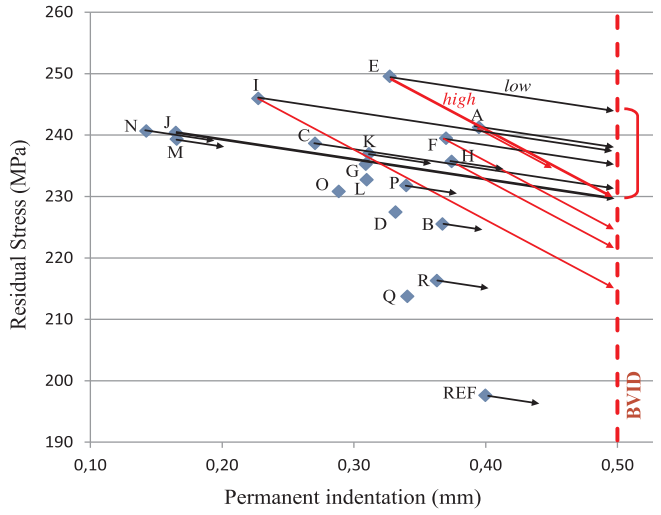


Fig. 14. "Best candidates" method applied to the 19 laminates, from 25 J energy.

important to put into perspectives the results of the optimization done with the DPM model. To the author's knowledge, the DPM is one of the most efficient models that can represent impact, impact induced damage (including PI), and CAI within the same model, with such a result quality: representativeness of mechanisms and values of impact force evolution, PI, CAI, etc. However, due to the great complexity of the phenomenon and of the model, one must not expect DPM model to give a very fine accuracy in the current state of virtual tools development. The model makes possible the ranking of laminates' residual strength (with a quite satisfactory accuracy). This is the most important point in the case of design optimization, to find the best structure. However, there is also a significant dispersion in experimental results that makes unnecessary the search for an extreme precision in the estimation of BVID energy level.

Anyway, nowadays, an experimental validation of the optimized laminate obtained by numerical design is still necessary.

5. Conclusion

Using the Discrete Ply Model, a numerical impact damage tolerance sizing is proposed. This work is possible thanks to the ability of the DPM in capturing main damage as fibre failure, matrix cracking and delamination from impact to CAI event. In the first part of the study, an experimental/numerical comparisons campaign was performed, showing quite accurate results in dent depth and residual strength prediction, two key parameters in this approach.

After this validation, the model was used to make a laminate design optimization with damage tolerance. In a first part, a reduced design space made of 19 laminates was proposed and full impact and CAI calculations were done at different impact energy level around the energy necessary to obtain a visible damage equal to BVID. Simple interpolations were then done to determine the best laminates in terms of damage tolerance strength, showing the ability of DPM to make a composite design optimization with damage tolerance. However, within the 19 samples studied, no clear rule or trend emerges to justify the impact damage tolerance of a given stacking sequence. This result again underlines the importance of numerical simulations development for composite damage prediction, as no practical rules can be established for an industrial use.

The principle of a classical optimization loop, more time-efficient, was also presented, but not applied here, the objective of the study being to study the evolution of CAI residual stress versus permanent indentation curves in order to propose an improved approach.

This approach is based on the knowledge of an approximate linear decrease of CAI stress when permanent indentation increases. It enables, from a single full impact and CAI calculation for all studied laminate, a rough estimation of the CAI strength. Thus, it is possible to define a reduced set of "best candidates" to perform a finer optimization. This enables reduction of computation time, which is a critical point in composite numerical simulations.

However, even with this reduction of the global number of simulations to perform during design optimization, the 36 h duration (on 20 CPUs) for a single impact and CAI simulation is still too high to be applied to more industrial design spaces made of hundreds or thousands laminates. An effort to drastically reduce models calculation time has to be done.

Acknowledgments

Authors would like to gratefully acknowledge CALMIP (CALcul en Midi-Pyrénées) for access to the HPC resources under the allocation p1026.

References

[1] Tropis A, Thomas M, Bounie JL, Lafon P. Certification of the composite outer wing of the ATR72. J Aerosp Eng 1994;209:327–39.
[2] Huang KY, De Boer A, Akkerman R. Analytical modeling of impact resistance and damage tolerance of laminated composite plates. AIAA J 2008;46(11):2760–72.
[3] Combes RC. Design for damage tolerance. J Aircraft 1970;7(1):18–20.
[4] Abrate S. Impact on Composites Structures. Cambridge University Press; 1998.
[5] Eve O. Etude du comportement des structures composites endommagées par impact basse vitesse PhD Thesis France: University of Metz; 1999
[6] Richardson MOW, Wisheart MJ. Review of low-velocity impact properties of composite materials. Compos A 1996;27(12):1123–31.
[7] Cantwell WJ, Morton J. The impact resistance of composite materials – a review. Composites 1991;22(5):347–62.
[8] Feraboli P, Kedward KT. Enhanced evaluation of the low-velocity impact response of composite plates. AIAA J 2004;42(10):2143–52.
[9] Pilchak AL, Uchiyama T, Liu D. Low velocity impact response of small-angle laminated composites. AIAA J 2006;44(12):3080–7.
[10] Olsson R. Analytical prediction of large mass impact damage in composite laminates. Compos A 2001;32:1207–15.
[11] Zhou G. The use of experimentally-determined impact force as damage measure in impact damage resistance and tolerance of composite structures. Compos Struct 1998;42:375–82.
[12] Suemasu H, Kumagai T, Gozu K. Compressive behavior of multiply delaminated composite laminates part 1: experiment and analytical development. AIAA J 1998;36(7):1279–85.
[13] Suemasu H, Kumagai T. Compressive behavior of multiply delaminated composite laminates part 2: finite element analysis. AIAA J 1998;36(7):1286–90.
[14] Rouchon J. Certification of Large Aircraft Composite Structures, Recent Progress and New Trends in Compliance Philosophy, 17th ICAS, Stockholm, Sweden, 1990.
[15] Acar E, Haftka RT, Kim NH. Effects of structural tests on aircraft safety. AIAA J 2010;48(10):2235–48.
[16] Lopes CS, Camanho PP, Gurdal Z, Maimi P, Gonzalez EV. Low-Velocity impact damage on dispersed stacking sequence laminates. Part II: numerical simulations. Compos Sci Technol 2009;69(7–8):937–47.
[17] Menna C, Asprone D, Caprino G, Lopresto V, Prota A. Numerical simulation of impact tests on GFRP composite laminates. Int J Impact Eng 2011;38:677–85.
[18] Lopes CS, Sadaba S, Gonzalez C, Lorca JL, Camanho PP. Physically-sound simulation of low-velocity impact on fiber reinforced laminates. Int J Impact Eng 2015;92:3–17.
[19] Schoeppner GA, Abrate S. Delamination threshold loads for low velocity impact on composite laminate. Compos A 2000;31:903–15.

[20] Shi Y, Swait T, Soutis C. Modelling damage evolution in composite laminate subjected to low velocity impact. Compos Struct 2012;94(9):2902–13.
[21] Elder DJ, Thomson RS, Nguyen MQ, Scott ML. Review of delamination predictive methods for low speed impact of composite laminates. Compos Struct 2004;66(1–4):677–83.
[22] Lammerant L, Verpoest I. Modelling of the interaction between matrix cracks and delaminations during impact of composite plates. Compos Sci Technol 1996;56(10):1171–8.
[23] Li S, Reid SR, Zou Z. Modelling damage of multiple delaminations and transverse matrix cracking in laminated composites due to low velocity lateral impact. Compos Sci Technol 2006;66:827–36.
[24] Razi H, Kobayashi AS. Delamination in cross-ply laminated composite subjected to low-velocity impact. AIAA J 1993;31(8):1498–502.
[25] de Moura MFSF, Gonçalves JPM. Modelling the interaction between matrix cracking and delamination in carbon–epoxy laminates under low velocity impact. Compos Sci Technol 2004;64:1021–7.
[26] Bachrach WE, Hansen RS. Mixed finite-element method for composite cylinder subjected to impact. AIAA J 1989;27(5):632–8.
[27] Hallett SR, Jiang WG, Khan B, Wisnom MR. Modelling the interaction between matrix cracks and delamination damage in scaled quasi-isotropic specimens. Compos Sci Technol 2008;68(1):80–9.
[28] Aslan Z, Sahin M. Buckling behaviour and compressive failure of composite laminates containing multiple large delaminations. Compos Struct 2009;89:382–90.
[29] Dang TD, Hallett SR. A numerical study on impact and compression after impact behavior of variable angle tow laminates. Compos Struct 2013;96:194–206.
[30] Dugdale DS. Yielding of steel sheets containing slits. J Mech Phys Solids 1960;8:100–8.
[31] Makhecha DP, Kapania RK, Johnson ER, Dillard DA. Dynamic fracture analysis of adhesively bonded joints using explicit methods. AIAA J 2007;45(11):2778–84.
[32] Barenblatt GI. The mathematical theory of equilibrium of cracks in brittle fracture. Adv Appl Mech 1962;7:55–129.
[33] Faggiani A, Falzon BG. Predicting low-velocity impact damage on a stiffened composite panel. Compos A 2010;41(6):737–49.
[34] Iarve EV, Gurvich MR, Mollenhauer DH, Rose CA, Davila CG. Mesh-independent matrix cracking and delamination modeling in laminated composites. Int J Numer Methods Eng 2011;88:749–73.
[35] Turon A, Camanho PP, Costa J, Renart J. Accurate simulation of delamination growth under mixed-mode loading using cohesive elements: Definition of interlaminar strengths and elastic stiffness. Compos Struct 2010;92:1857–64.
[36] Harper PW, Sun L, Hallett SR. A study on the influence of cohesive zone interface element strength parameters on mixed mode behavior. Compos A 2012;43:722–34.
[37] Donadon MV, Iannucci L, Falzon BG, Hodgkinson JM, de Almeida SFM. A progressive failure Model for composite laminates subjected to low velocity impact damage. Comput Struct 2008;86:1232–52.
[38] Bouvet C, Castanié B, Bizeul M, Barrau JJ. Low velocity impact modelling in laminate composite panels with discrete interface elements. Int J Solids Struct 2009;46(14–15):2809–21.
[39] Gonzalez EV, Maimi P, Camanho PP, Turon A, Mayug JA. Simulation of drop-weight impact and compression after impact tests on composite laminates. Compos Struct 2012;91(11):3364–78.
[40] Tan W, Falzon BG, Chiu LNS, Price M. Predicting low velocity impact damage and Compression-After-Impact (CAI) behavior of composite laminates. Compos A 2015;71:212–26.
[41] Panettieri E, Fanteria D, Danzi F. Delamination growth in compression after impact test simulations: Influence of cohesive elements parameters on numerical results. Compos Struct 2016;137:140–7.
[42] Wardle BL, Lagace PA. On the use of dent depth as an impact damage metric for thin composite structures. J Reinf Plast Compos 1997;16(12):1093–110.
[43] Chen P, Shen Z, Xiong J. Failure mechanisms of laminated composites subjected to static indentation. Compos Struct 2006;75(1–4):489–95.
[44] Bouvet C, Rivallant S, Barrau JJ. Low velocity impact modeling in composite laminates capturing permanent indentation. Compos Sci Technol 2012;72(16):1977–88.
[45] He W, Guan Z, Li X, Liu D. Prediction of permanent indentation due to impact on laminated composites based on an elasto-plastic model incorporating fiber failure. Compos Struct 2013;96:232–42.
[46] Hongkarnjanakul N, Bouvet C, Rivallant S. Validation of low velocity impact modeling on different stacking sequences of CFRP laminates and influence of fibre failure. Compos Struct 2013;106:549–59.
[47] Rivallant S, Bouvet C, Hongkarnjanakul N. Failure analysis of CFRP laminates subjected to Compression After Impact : FE simulation using discrete interface elements. Compos A 2013;55:83–93.
[48] Israr HA, Rivallant S, Barrau JJ. Experimental investigation on mean crushing stress characterization of carbon-epoxy plies under compressive crushing mode. Compos Struct 2013;96:357–64.
[49] ASTM /D7136M, “Standard Test Method for Measuring the Damage Resistance of a fiber-reinforced polymer matrix composit to a drop-weight impact event,” ASTM editor, 2015.
[50] ASTM D7137/D7137M, “Standard Test Method for Compressive Residual Strength Properties of Damaged Polymer Matrix Composite Plates,” ASTM editor, 2012.